**Aalborg Universitet**

**AALBORG UNIVERSITY**

DENMARK

**Comparison of Transient Behaviors of Wind Turbines with DFIG Considering the Shaft Flexible Models**

Chen, Zhe; Ye, Ren-jie; Hui, Li; Gao, Qiang

# Comparison of Transient Behaviors of Wind Turbines with DFIG Considering the Shaft Flexible Models

Ren-jie Ye [1], Hui Li [1], Zhe Chen [2], Qiang Gao[1]

[1] State Key Laboratory of Power Transmission Equipment & System Security and New Technology,
Chongqing University, China

[2] Institute of Energy Technology, Aalborg University, Denmark

*Abstract*- **In order to investigate the impacts of the integration of wind farms into utilities network, it is necessary to analyze the transient performances of wind power generation systems. In this paper, an assessment of the impact that the different representations of drive-train dynamics have on the electrical transient performances of doubly fed induction generator (DFIG) wind turbines with different operationally states is investigated. In order to compare the transient performances of DFIG wind turbines during electrical transients, a DFIG model with simple one-mass lumped model and a two-mass shaft flexible model of wind turbine drive train systems are presented including the control strategies of the grid side and rotor side converters. The transient performances of DFIG wind turbines are evaluated under super- and sub-synchronous operation during different grid voltage dips. Simulation results have shown that it is needed to consider two mass shaft flexible model for the sake of exact analysis of transient behavior of DFIG wind turbines, especially when a more serious grid voltage dips occurs in power system and DFIG is at super-synchronous operation.**

## I. INTRODUCTION

In recent years, large wind turbines with the rated power of MW levels are becoming more and more attractive in order to extract more power from wind [1]. As the wind turbine size increases, the flexibility associated with the wind turbine drive train system also increases and so does the influences that it has on the electrical transient performance of the wind turbine. In addition, as the penetration of wind power continually increases, more wind turbines are required to stay in grid connected during a grid fault. So, increasing levels of wind turbine generation in modern power system is initiating a need for accurate wind generation transient stability models.

Doubly fed induction generators (DFIG) are popular configurations for large wind generator systems. The stator of DFIG connects the grid directly and provides for variable speed operation by using a partially rated converter on the rotor side, so it is a common choice for its smaller converter capacity than other VSCF generators by a number of manufactures of large wind turbines.

There are a few reports investigating the transient models of DFIG wind turbines for the transient performance studies [2]-[14], however, the transient models are mainly focused on different machine models of DFIG for some papers. For example, an 8th-order generator model is derived in [2]. A 3rd-order, 5th-order and 8th-order models are built and compared in [3] for the transient performance studies, the results have shown there may be a few discrepancy with different detailed generator models, however, the more complicated generator models may be not applicable to study the transient performance of the large wind power systems. In addition, the drive train system of the wind turbine is usually used by a simple one-mass lumped model for its transient stability analysis; however, the shaft flexibility may become obvious with the increase of capacity of the wind turbine system. For the sake of exact analysis of transient performances of DFIG system for wind power generation, it is needed to consider the flexible effect of the wind turbine drive-train shaft system.

In this paper, an assessment of the impact that the representation of wind turbine drive train dynamics has on the electrical transient performances of DFIG wind turbines is investigated. A two-mass model taking the shaft flexibility into account in the structural dynamics is presented. In order to compare the transient performance of DFIG wind turbines with different drive-train system model, the transient response of DFIG with rated power 3MW are investigated under super- and sub-synchronous operation during grid different voltage dips.

## II. DYNAMIC MODELS OF DFIG WIND TURBINES
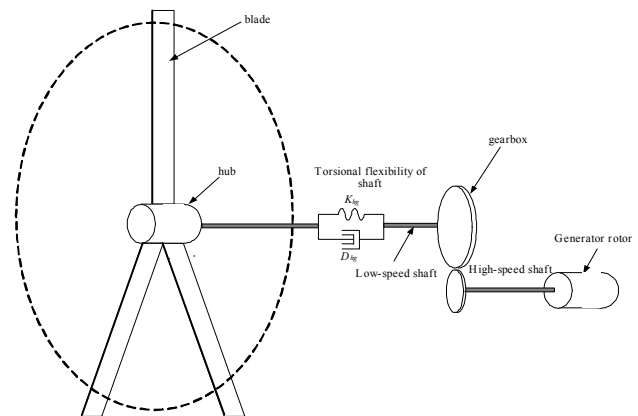
### A. Models of Drive-train System



Fig. 1 Schematic diagram of the drive train of a wind turbine system

(a) a two-mass equivalent model    (b) a one-mass equivalent model
Fig. 2 Schematic diagrams of the one-mass and two-mass equivalent models of a wind turbine

Fig. 1 illustrates the main rotor structural components of a wind turbine, namely blades, hub, low-speed shaft, gearbox, high-speed shafts and generator rotor [9].

Modeling of a wind turbine drive train system is a complicated one. According to the blade element theory, modeling of blade and shafts needs complicated and lengthy computations [9]. Moreover, it also dependents on the detailed and accurate information about the rotor geometry. For that reason, considering only the transient events of the wind generator system, an equivalent lump mass modeling method of wind turbine system is normally used. In this method, the model of the drive-train system can be built consists of two masses, i.e. turbines mass and generator mass. The two masses are connected to each other with a shaft that has a certain stiffness and damping constant value. Fig.2 (a) shows the schematic diagrams of two-mass equivalent model of a wind turbine.

The equation of this model is given as:

$$\begin{cases} 2H_w \dfrac{d\omega_w}{dt} = T_w - K_s\theta_s - D_s(\omega_w - \omega_g) - D_w\omega_w \\ 2H_g \dfrac{d\omega_g}{dt} = K_s\theta_s - T_e + D_s(\omega_w - \omega_g) - D_g\omega_g \\ \dfrac{d\theta_s}{dt} = \omega_0(\omega_w - \omega_g) \end{cases} \quad (1)$$

Where $H$ is the inertia constant, $T$ is torque and $\omega$ is angular speed. Subscripts $g$ and $w$ indicate the generator and turbine quantities, respectively. The shaft stiffness and damping constant value are represented in $K_S$ and $D_s$, $\omega_0$ is the base value of angular speed. All the quantities are in per unit value.

In order to make a comparison of the transient stability analysis of the wind generator system with different equivalent models of the mechanical system, the traditional one-mass shaft lumped model has been considered, which are shown in Fig. 2(b). The equation of this model can be given as:

$$2H_M \frac{d\omega_M}{dt} = T_w - T_e - D_M\omega_M \quad (2)$$

Where $H_M$ is the inertia constant, $D_M$ is the damping constant value of turbine. $\omega_M$ is the angular speed of generator. Of cause, in this model the angular speed of turbine is equal to the angular speed of generator.

*B. Control Strategy of Grid-side Converter*

A vector-control approach is used with a reference frame oriented along the grid voltage vector position, enabling independent control of the active and reactive power flowing between the grid and the grid-side converter. The PWM voltage source converter is current regulated, with the d-axis current



Fig.3 Grid-side PWM voltage source converter arrangement to the grid/transformer



Fig.4 Vector-control structure for grid-side PWM voltage source converter used to regulate the DC-link voltage and the q-axis current used to regulate the reactive power.

Fig.3 shows the schematic of the grid-side PWM voltage source converter, where $u_{gabc}$ are the three phase grid voltages, $u_{gcabc}$ are the three phase grid-side converter voltages, $i_{ga}$, $i_{gb}$, $i_{gc}$ are the three phase grid-side converter currents, $R_g$ and $L_g$ are the inductor resistance and inductance, $i_{dcg}$, $i_{dcr}$ are the grid-side and rotor-side DC currents, $C$ is the DC-link capacitor.

The voltage balance across the inductor is:

$$\begin{bmatrix} u_{ga} \\ u_{gb} \\ u_{gc} \end{bmatrix} = R_g \begin{bmatrix} i_{ga} \\ i_{gb} \\ i_{gc} \end{bmatrix} + L_g \frac{d}{dt}\begin{bmatrix} i_{ga} \\ i_{gb} \\ i_{gc} \end{bmatrix} + \begin{bmatrix} u_{gca} \\ u_{gcb} \\ u_{gcc} \end{bmatrix} \quad (3)$$

By using the abc-to-dq transformation matrix, the following equation can be given:

$$\begin{cases} u_{gd} = R_g i_{gd} + L_g \dfrac{di_{gd}}{dt} - \omega_e L_g i_{gq} + u_{gcd} \\ u_{gq} = R_g i_{gq} + L_g \dfrac{di_{gq}}{dt} + \omega_e L_g i_{gd} + u_{gcq} \end{cases} \quad (4)$$

where $u_{gd}$, $u_{gq}$ are the grid voltages in d- and q-axis, $u_{gcd}$, $u_{gcq}$ are the grid-side converter voltages in d- and q-axis, $i_{gd}$, $i_{gq}$ are the grid-side converter currents in d- and q-axis, $\omega_e$ is the electrical. angular velocity of the grid voltage.

Neglecting harmonics due to the switching and the losses in the resistance and converter, the following equations can be obtained [15]:

$$\begin{cases} u_{dc}i_{dcg} = \dfrac{3}{2}u_{gd}i_{gd} \\ u_{gd} = \dfrac{m}{2}u_{dc} \\ i_{dcg} = \dfrac{3}{4}mi_{gd} \\ C\dfrac{du_{dc}}{dt} = i_{dcg} - i_{dcr} \end{cases} \tag{5}$$

where $m$ is the PWM modulation depth of the grid-side converter.

By using the control strategy described in (5), it can be seen that the DC-link voltage can be controlled via $i_{gd}$.

The currents $i_{gd}$ and $i_{gq}$ can be regulated by using $u_{gcd}$ and $u_{gcq}$ respectively. The control scheme thus utilises current control loops for $i_{gd}$ and $i_{gq}$, with the $i_{gd}$ demand being derived from the DC-link voltage error. The $i_{gq}$ demand determines the reactive power flow between the grid and the grid-side converter. Normally the $i_{gq}$ reference value may be set to zero, which ensures zero reactive power exchange between the grid and the grid-side converter.

The vector-control scheme for grid-side PWM voltage source converter is shown in Fig.4, where $u_{gcabc}^*$ are the reference values of the three phase grid-side converter voltages, $u_{gcd}^*, u_{gcq}^*$ are the reference values of the grid-side converter voltages in d- and q-axis, $i_{gd}^*, i_{gq}^*$ are the reference values of the grid-side converter currents in d- and q-axis.

### C. Control Strategy of Rotor-side Converter

A detailed model of DFIG which includes electromagnetic transients both in the stator and the rotor circuits is used when performing the transient stability studies. According to a standard per-unit notation [8, 9], in a reference frame rotating at synchronous speed and taking the motor convention, the transient models of grid-connected DFIG can be represented by the detailed differential equations of the flux linkages:

$$\begin{cases} u_{sd} = R_s i_{sd} + \dfrac{d\psi_{sd}}{dt} - \omega_s\psi_{sq} \\ u_{sq} = R_s i_{sq} + \dfrac{d\psi_{sq}}{dt} + \omega_s\psi_{sd} \\ u_{rd} = R_r i_{rd} + \dfrac{d\psi_{rd}}{dt} - s\omega_s\psi_{rq} \\ u_{rq} = R_r i_{rq} + \dfrac{d\psi_{rq}}{dt} + s\omega_s\psi_{rd} \end{cases} \tag{6}$$

The equations of flux linkage is given as：

$$\begin{cases} \psi_{sd} = L_s i_{sd} + L_m i_{rd} \\ \psi_{sq} = L_s i_{sq} + L_m i_{rq} \\ \psi_{rd} = L_r i_{rd} + L_m i_{sd} \\ \psi_{rq} = L_r i_{rq} + L_m i_{sq} \end{cases} \tag{7}$$

Where $\omega_s$ is the synchronous speed；$u, \psi, I, R, L$ are the voltage, flux linkage, current, resistance and inductance；$L_m$ is the inductance between rotor and stator；subscript $s$、$r$ indicate the stator and rotor of electric machine, respectively；subscript $d, q$ indicate the d, q components, respectively；$s$ is slip ratio of DFIG.

The active and reactive power of stator can be given as:

$$\begin{cases} P_s = \dfrac{3}{2}\left(u_{sd}i_{sd} + u_{sq}i_{sq}\right) \\ Q_s = \dfrac{3}{2}\left(u_{sq}i_{sd} - u_{sd}i_{sq}\right) \end{cases} \tag{8}$$

In order to implements the active and reactive power decoupling control of DFIG, in this paper, we adopt stator voltage oriented rotor current control. It means that, $u_{sd}=U_s$, $u_{sq}=0$.

The stator active and reactive power can be given as：

$$\begin{cases} P_s = -\dfrac{3L_m U_s i_{rd}}{2L_s} \\ Q_s = \dfrac{3}{2}\left(\dfrac{U_s^2}{\omega_s L_s} + \dfrac{U_s L_m i_{rq}}{L_s}\right) \end{cases} \tag{9}$$

The electromagnetic torque is given as：

$$T_e = -n_p\frac{L_m}{L_s}\vec{\psi}_s \times \vec{i}_r = -n_p\frac{L_m}{L_s}\psi_s i_{rd} \tag{10}$$

Fig.5 shows the vector-control scheme for rotor-side PWM voltage source converter, where $u_{abcr}^*$ are the reference values of the three phase rotor voltages, $u_{rd}^*, u_{rq}^*$ are the reference values of the rotor voltages in d- and q-axis, $i_{rd}^*, i_{rq}^*$ are the reference values of the rotor currents in d- and q-axis. Stator active and reactive power can be controlled by regulating the d, q-axis components of rotor current, which are shown in Fig.5.

$$\begin{cases} \Delta u_{rd} = R_r i_{rd} - s\omega_s(L_r i_{rq} + L_m i_{sq}) \\ \Delta u_{rq} = R_r i_{rq} + s\omega_s(L_r i_{rd} + L_m i_{sd}) \end{cases} \tag{11}$$
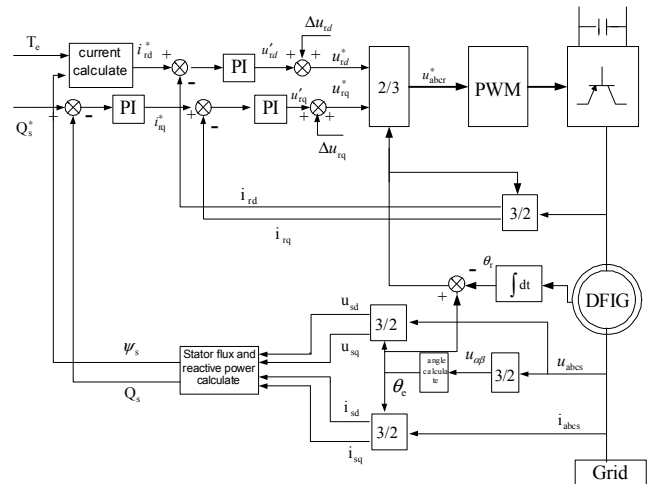


Fig.5 Control structure of rotor-side's active and reactive power decoupling control
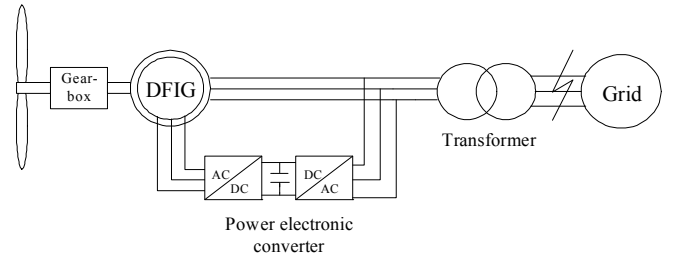


Fig.6 Schematic diagram of a grid connected DFIG wind turbine system

## III. SIMULATION OF TRANSIENT RESPONSES OF DFIG BASED ON DIFFERENT EQUIVALENT MODEL

Fig.6 shows the schematic diagram of the grid connected DFIG wind turbine system during grid voltage fault. In the following simulation, the input mechanical torque keeps a constant during a grid voltage drop, which means pitch control system will be not action. In addition, the rotor side converter is assumed to ride through the fault current even though for a thee-phase short-circuit fault at the stator terminals of DFIG. The main parameters of DFIG wind turbine system are shown as Table I.

In order to show the effects of the different drive-train system models on the transient performances of DFIG wind turbine, the transient performances are simulated with different grid voltage drops and different operational generator speed. In the following simulation, three cases have been investigated for a 40% and 80% gird voltage drops under a super-synchronous and sub-synchronous generator speed.

### A . 40% Voltage Dip under Super-synchronous Operation

In this case, the symmetrical three-phase stator voltage drops 40% at t=0.05s, and at t=0.15s the voltage is restored to its pre-sag value. Before the grid fault occurs, the generator rotor speed is set 1.2 per unit.

Fig.7 shows the transient behaviors of this case. As it can be seen from Fig.7(a) that the active power has a larger oscillation during the post-fault for the two-mass shaft system model in comparison with a single mass model. For example, the maximal active power will be 1.1 pu considering a two-mass model when the grid voltage fault clears, however, this value is only 0.85pu for the one-mass model. In addition, the reactive power has been rarely affected by different shaft system modeling. As it can be seen from Fig.7(c) that the angular speed of DFIG rotor has a larger oscillation during the post-fault for the two-mass shaft system model in comparison with a single mass model. For example, the maximal angular speed of rotor will be 1.219pu considering a two-mass model when the grid voltage fault clears, however, this value is only 1.203pu for the one-mass model, the angular speed of rotor keeps oscillating until t=3.5s for the two-mass model when the grid voltage fault clears, however, at t=0.25s the angular speed of rotor is restored to its pre-sag value of the one-mass model. Furthermore, the torsional torque has a large oscillation with a two-mass model.
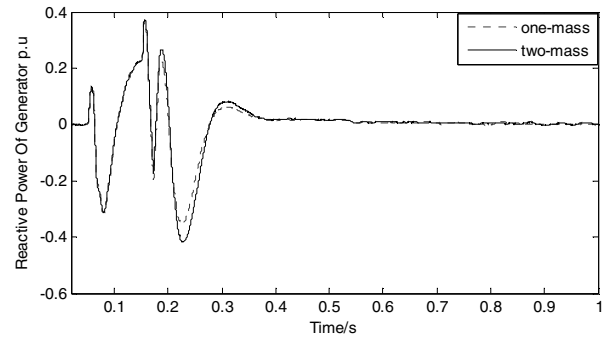
TABLE I
MAIN PARAMETERS OF DFIG WIND TURBINE SYSTEM

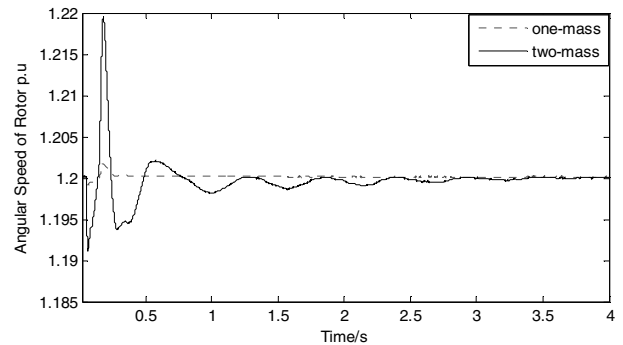| Main parameters | Value |
|---|---|
| Wind turbine | |
| Per unit inertia constant of hub $H_w$ (s) | 4.54 |
| Torsional stiffness of low-speed shaft $K_s$ (p.u./el.rad) | 0.3 |
| DFIG system | |
| Normal power base (MW) | 3 |
| Voltage base $U_N$(V) | 575 |
| Stator resistance $R_s$ (p.u.) | 0.0071 |
| Rotor resistance $R_r$ (p.u.) | 0.005 |
| Stator leakage inductance $X_{s\sigma}$ (p.u.) | 0.171 |
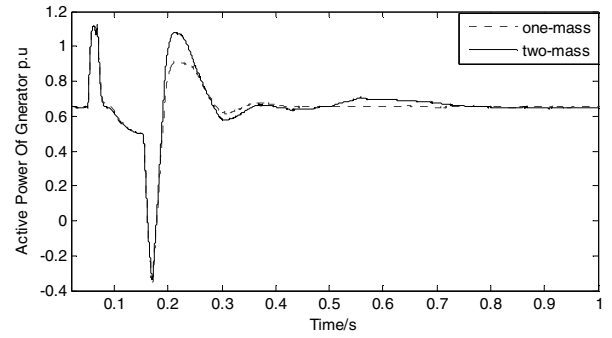


(a) Active power responses
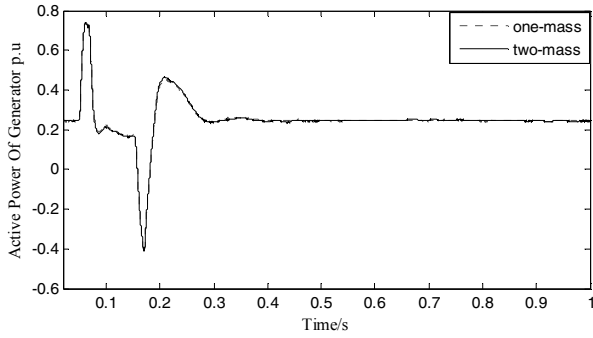


(b) Reactive power responses
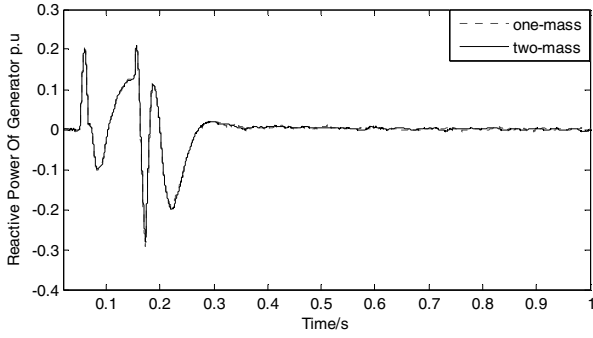


(c) Angular speed of rotor responses
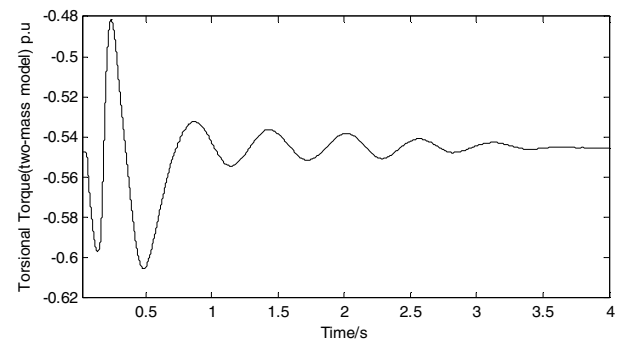


(d) Torsional torque responses

Fig.7 Transient responses of 40% dip under super-synchronous operation

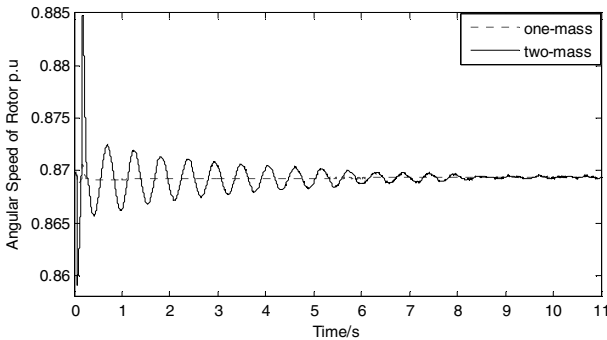### B. 40% Voltage Dip under Sub-synchronous Operation

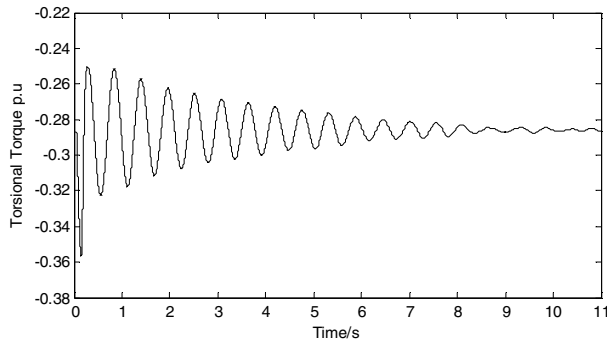In this case, symmetrical three-phase stator voltage drops

(a) Active power of generator responses


(b) Reactive power of generator responses


(c) Angular speed of rotor responses


(d) Torsional torque responses

Fig.8 Transient responses of 40% dip under sub-synchronous operation

40% at t=0.05s, and at t=0.15s the voltage is restored to its pre-sag value. Before the grid fault occurs, the generator rotor speed is set 0.87 per unit.

As it can be seen from Fig.8(a) and Fig.8(b), the active power and reactive power have been rarely affected by different shaft system modeling. In addition, the angular speed of rotor and the

torsional torque have a larger oscillation during the post-fault for the two-mass shaft system model in comparison with a single mass model, as it can be seen from Fig.8(c) and Fig.8(d). For example, the angular speed of rotor and the torsional torque are keep oscillating until t=11s for the two-mass model when the grid voltage fault clears, however, at t=0.25s the angular speed of rotor is restored to its pre-sag value of the one-mass model.
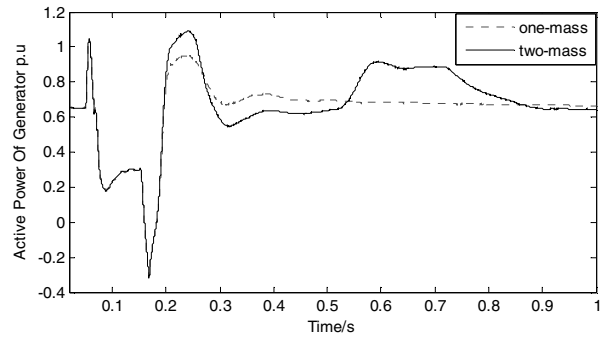
C. 80% Voltage Dip under Super-synchronous Operation

In this case, the symmetrical three-phase stator voltage drops 80% at t=0.05s, and at t=0.15s the voltage is restored to its pre-sag value. Before the grid fault occurs, the generator rotor speed is set 1.2 per unit.

As it can be seen from Fig.9(a), the active power has a larger oscillation during the post-fault for the two-mass shaft system model in comparison with a single mass model. For example, the maximal active power will be 1.1pu considering a two-mass model when the grid voltage fault clears, however, this value is only 0.85pu for the one-mass model. The second peak value of active power will be 0.915pu considering a two-mass model during the post-fault, however, this value is only 0.707pu for the case voltage drops 40%.

As it can be seen from Fig.9(c) that the maximal angular speed of rotor will be 1.24pu considering a two-mass model when the grid voltage fault clears, which is larger than the value of the case voltage drops 40%. In addition, at t=3.5s the angular speed of rotor is not restored to steady operation.
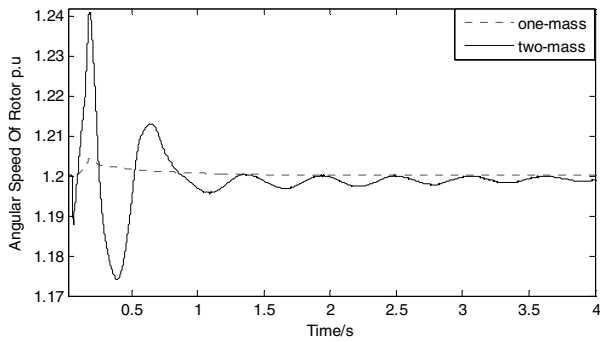
Fig.9(d) shows that the maximal torsional torque will be -0.2pu, this value is -0.48pu for the case voltage drops 40%. At t=3.5s the torsional torque is not restored to steady operation.
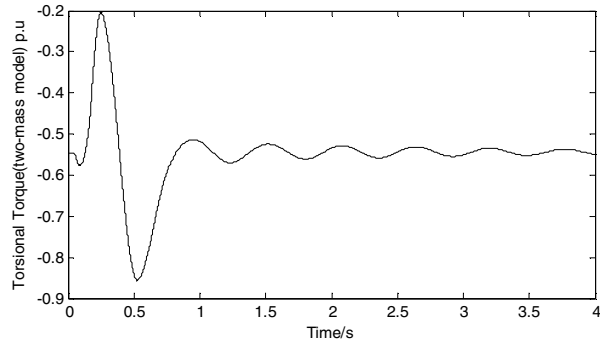

(a) Active power of generator responses
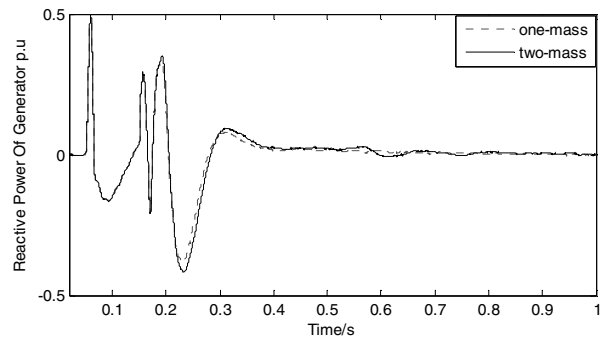

(b) Reactive power of generator responses

(c) Angular speed of rotor responses



(d) Torsional torque responses

Fig.9 Transient responses of 80% dip under super-synchronous operation

## IV. CONCLUSIONS

In order to evaluate the effect of the drive train system flexibility on the transient performances for the wind turbine with DFIG, both a one-mass lumped model and a two-mass shaft flexible model are presented. The control strategies of grid side converter and rotor side converter of DFIG are also described. The DFIG system models with different shaft models have been developed in this paper. Based on the two different models, the transient behaviors are simulated and compared when the different voltage sags occur under the conditions of different generator speed operations. The simulation results have shown the wind turbines system model incorporating the two-mass shaft model may be important to the transient performance analysis exactly. At the same grid voltage drop, if the initiation generator speed is higher, the active and reactive power have a larger oscillation. However, in the low speed, the variation time of the generator speed and the torsional torque of the shaft system may be longer. In addition, at the same initiation operation speed, the transient response have a larger oscillation with a more serious voltage drop.

## ACKNOWLEDGMENT

## REFERENCES

[1] http://www.gwec.net/uploads/media/07_02_PR_Global_Statistics_2006.pdf

[2] LI Dong, and CHEN Chen, "A study on dynamic model of wind turbine generator sets," *Proceeding of CSEE*, vol.25, no.3, pp.115-119, 2005(in Chinese).

[3] YIN Ming, LI Gengyin, ZHOU Ming, and ZHAO Chengyong, "Analysis and comparison of dynamic models for the doubly fed induction generator wind turbine," *Automation of Electric Power Systems*, vol.30, no.13, pp. 22-27, 2006.

[4] LIU Qihui, HE Yikang, and ZHANG Janhua, "Operation control and modeling simulation of ac-excited variable-speed constant-frequency (AVESCF) wind power generator," *Proceedings of the CSEE*, vol.26, no.5, pp.43-50, 2006(in Chinese)

[5] Xiao Jinsong, Ni Weidou, and Jiang Tong, "Modeling and simulation of large wind power generator set," *Acta Energiae Solaris Sinica*, vol.18, no.2, pp.117-127, 1997.

[6] T. Petru , and T. Thiringer, "Modeling of wind turbines for power system studies," *Power Systems,IEEE Transactions on*, vol.17 no.4, pp.1132-1139 2002

[7] SK. Salman, and J. T. .Anitul, "Windmill modeling consideration and factors influencing the stability of a grid-connected wind power-based embedded generator," *IEEE Trans, Power system*, vol.18, no.2, pp. 793-802 2003

[8] Chen Shuyong, Dai Huizhu, Bai Xiaomin et al, "Reliability model of wind power plants and its application," *Proceedings of the CSEE*, 2000, vol.20, no.3, pp.26-29.

[9] S.Seman, F.Iov , J.Niiranen and A.Arkkio, "Advanced modeling of doubly fed induction generator wind turbine under network disturbance," in *Proc.5th Int,workshop Large-scale Integration Wind Power Transmission Networks off shore Wind Farms.alasgow*,U.K,Apr.7-8,2005.pp.305_314H. LI, Z.J.

[10] Tao Sun, Z. Chen and F Blaabjerg, "Transient Analysis of Grid-Connected Wind Turbines with DFIG After an External Short-Circuit Fault,".*proc.Nordic Wind Power*,2004:1-6.

[11] Tao Sun, Z. Chen and F. Blaabjerg, "Transient Stability of DFIG Wind Turbines at an External Short-Circuit Fault" *Wind Energy*,2005,8:345-360

[12] J.B.Ekanayake, L.Holdsworth, X.G.Wu and N.Jenkins, "Dynamic modeling of doubly fed induction generator wind turbines," *IEEE.Transl, Power Syst*,vol.18.no.2.pp.803-809.May 2003

[13] Hui Li, Shunchang Yang and Yong Liao. "Studies on excitation control of power system voltage oriented for doubly fed generators connected to an infinite bus," in *Proceedings of CSEE*,2003,23(8):159-162(in Chinese)

[14] S.Seman,F.Iov, J.Niiranen, and A.Arkkio, "Advanced modeling of doubly fed induction generator wind turbines under network disturbance," In *Proc.5th Int, workshop Large-scale Integration Wind Power Transmission Networks off shore Wind Farms.alasgow*,U.K,Apr.7-8,2005.pp.305_314.

[15] R.Pena, J. C. Clare, and G. M. Asher. "Doubly fed induction generator using back-to-back PWM converters and its application to variable-speed wind-energy generation," *IEEE Proc.Electr.Power Appl.*, vol.143, no.3, pp.231-241, May 1996